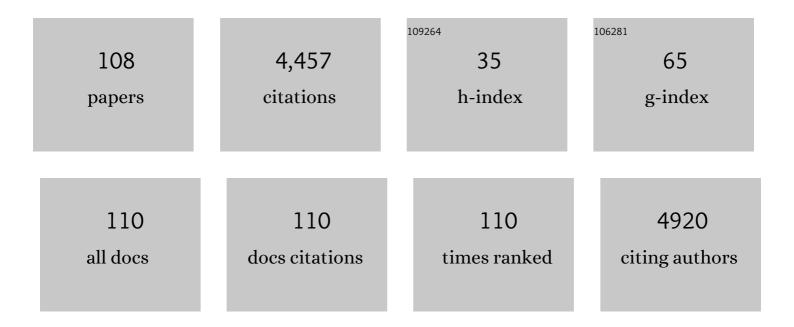
Jingxin Zhou

List of Publications by Year in descending order

Source: https://exaly.com/author-pdf/7406156/publications.pdf Version: 2024-02-01



#	Article	IF	CITATIONS
1	Graphene-based polymer composite films. , 2022, , 309-331.		0
2	Facile preparation and high performance of wearable strain sensors based on ionically cross-linked composite hydrogels. Science China Materials, 2021, 64, 942-952.	3.5	105
3	Green Preparation and Environmental Applications of Some Electrospun Fibers. Materials Horizons, 2021, , 455-484.	0.3	0
4	Self-Assembled Black Phosphorus-Based Composite Langmuir–Blodgett Films with an Enhanced Photocurrent Generation Capability and Surface-Enhanced Raman Scattering Properties. ACS Omega, 2021, 6, 4430-4439.	1.6	12
5	Preparation and aggregate state regulation of co-assembly graphene oxide-porphyrin composite Langmuir films via surface-modified graphene oxide sheets. Colloids and Surfaces A: Physicochemical and Engineering Aspects, 2020, 584, 124023.	2.3	71
6	In Situ Construction of Ag/TiO2/g-C3N4 Heterojunction Nanocomposite Based on Hierarchical Co-Assembly with Sustainable Hydrogen Evolution. Nanomaterials, 2020, 10, 1.	1.9	340
7	Facile Preparation and Highly Efficient Catalytic Performances of Pd-Cu Bimetallic Catalyst Synthesized via Seed-Mediated Method. Nanomaterials, 2020, 10, 6.	1.9	34
8	Chemical Vapor Deposition-Assisted Fabrication of Self-Assembled Co/MnO@C Composite Nanofibers as Advanced Anode Materials for High-Capacity Li-Ion Batteries. Langmuir, 2020, 36, 14342-14351.	1.6	6
9	Facile Fabrication of SrTiO ₃ @MoS ₂ Composite Nanofibers for Excellent Photodetector Application. Journal of Chemistry, 2020, 2020, 1-7.	0.9	3
10	Facile preparation of black phosphorus-based rGO-BP-Pd composite hydrogels with enhanced catalytic reduction of 4-nitrophenol performances for wastewater treatment. Journal of Molecular Liquids, 2020, 310, 113083.	2.3	22
11	Preparation and High Photocurrent Generation Enhancement of Self-Assembled Layered Double Hydroxide-Based Composite Dye Films. Langmuir, 2020, 36, 7483-7493.	1.6	12
12	Self-assembled functional components-doped conductive polypyrrole composite hydrogels with enhanced electrochemical performances. RSC Advances, 2020, 10, 10546-10551.	1.7	45
13	Fabrication of Hydrogels via Host–Guest Polymers as Highly Efficient Organic Dye Adsorbents for Wastewater Treatment. ACS Omega, 2020, 5, 5470-5479.	1.6	20
14	Facile Synthesis of Self-Assembled NiFe Layered Double Hydroxide-Based Azobenzene Composite Films with Photoisomerization and Chemical Gas Sensor Performances. ACS Omega, 2020, 5, 3689-3698.	1.6	44
15	Fabrication of hierarchical SrTiO ₃ @MoS ₂ heterostructure nanofibers as efficient and low-cost electrocatalysts for hydrogen-evolution reactions. Nanotechnology, 2020, 31, 205604.	1.3	47
16	Facile Preparation of Self-Assembled Black Phosphorus-Dye Composite Films for Chemical Gas Sensors and Surface-Enhanced Raman Scattering Performances. ACS Sustainable Chemistry and Engineering, 2020, 8, 4521-4536.	3.2	106
17	<scp><i>Morinda citrifolia</i></scp> (<scp>Noni</scp>) fruit juice promotes vascular endothelium function in hypertension via glucagonâ€like peptideâ€l <scp>receptor aMKKβâ€AMPKâ€eNOS</scp> pathwa Phytotherapy Research, 2020, 34, 2341-2350.	ay2.8	15
18	Controllable morphology and highly efficient catalytic performances of Pd–Cu bimetallic nanomaterials prepared via seed-mediated co-reduction synthesis. Applied Surface Science, 2020, 527, 146719.	3.1	19

#	Article	IF	CITATIONS
19	Facile Synthesis of Cu2O nanoparticle-loaded Carbon Nanotubes Composite Catalysts for Reduction of 4-Nitrophenol. Current Nanoscience, 2020, 16, 617-624.	0.7	24
20	The Role of Intestinal Fungi and Its Metabolites in Chronic Liver Diseases. Gut and Liver, 2020, 14, 291-296.	1.4	7
21	Hierarchical electrospun nanofibers treated by solvent vapor annealing as air filtration mat for high-efficiency PM2.5 capture. Science China Materials, 2019, 62, 423-436.	3.5	136
22	Self-assembled polyelectrolyte-based composite hydrogels with enhanced stretchable and adsorption performances. Journal of Molecular Liquids, 2019, 294, 111576.	2.3	26
23	Self-assembled hydrogels constructed via host-guest polymers with highly efficient dye removal capability for wastewater treatment. Colloids and Surfaces A: Physicochemical and Engineering Aspects, 2019, 579, 123670.	2.3	21
24	Preparation of Palladium Nanoparticles Decorated Polyethyleneimine/Polycaprolactone Composite Fibers Constructed by Electrospinning with Highly Efficient and Recyclable Catalytic Performances. Catalysts, 2019, 9, 559.	1.6	78
25	Preparation and Cu(II) ion removal capacities of Schiff base-based polystyrene nanocomposites for wastewater treatment. Integrated Ferroelectrics, 2019, 197, 49-57.	0.3	0
26	Facile Preparation of Hierarchical AgNP-Loaded MXene/Fe ₃ O ₄ /Polymer Nanocomposites by Electrospinning with Enhanced Catalytic Performance for Wastewater Treatment. ACS Omega, 2019, 4, 1897-1906.	1.6	234
27	Facile Preparation of Self-Assembled Polydopamine-Modified Electrospun Fibers for Highly Effective Removal of Organic Dyes. Nanomaterials, 2019, 9, 116.	1.9	78
28	Fabrication and Highly Efficient Dye Removal Characterization of Beta-Cyclodextrin-Based Composite Polymer Fibers by Electrospinning. Nanomaterials, 2019, 9, 127.	1.9	82
29	Facile solvothermal preparation of Fe ₃ O ₄ –Ag nanocomposite with excellent catalytic performance. RSC Advances, 2019, 9, 878-883.	1.7	64
30	Facile preparation of self-assembled hydrogels constructed from poly-cyclodextrin and poly-adamantane as highly selective adsorbents for wastewater treatment. Soft Matter, 2019, 15, 6097-6106.	1.2	105
31	Non-covalent self-assembly of multi-target polystyrene composite adsorbent with highly efficient Cu(II) ion removal capability. Colloids and Surfaces A: Physicochemical and Engineering Aspects, 2019, 577, 674-682.	2.3	10
32	MiR-889 promotes cell growth in human non-small cell lung cancer by regulating KLF9. Gene, 2019, 699, 94-101.	1.0	14
33	Haptoglobin 2-2 Genotype is Associated with More Advanced Disease in Subjects with Non-Alcoholic Steatohepatitis: A Retrospective Study. Advances in Therapy, 2019, 36, 880-895.	1.3	7
34	Facile Preparation of Carbon Nanotube-Cu2O Nanocomposites as New Catalyst Materials for Reduction of P-Nitrophenol. Nanoscale Research Letters, 2019, 14, 78.	3.1	74
35	Mg3Y2Ge3O12:Bi3+ UV fluorescent phosphor as the TiO2 "sensitizer―for enhancing the heavy oil viscosity reduction. Ceramics International, 2019, 45, 13112-13118.	2.3	3
36	Preparation and Dye Degradation Performances of Self-Assembled MXene-Co ₃ O ₄ Nanocomposites Synthesized via Solvothermal Approach. ACS Omega, 2019, 4, 3946-3953.	1.6	74

#	Article	IF	CITATIONS
37	Facile preparation and catalytic performance characterization of AuNPs-loaded hierarchical electrospun composite fibers by solvent vapor annealing treatment. Colloids and Surfaces A: Physicochemical and Engineering Aspects, 2019, 561, 283-291.	2.3	97
38	Self-assembled Graphene/Graphene Oxide-Based Nanocomposites Toward Photodynamic Therapy Applications. , 2018, , 227-254.		1
39	Selective Cu(II) ion removal from wastewater via surface charged self-assembled polystyrene-Schiff base nanocomposites. Colloids and Surfaces A: Physicochemical and Engineering Aspects, 2018, 545, 60-67.	2.3	66
40	Fabrication of tunable hierarchical MXene@AuNPs nanocomposites constructed by self-reduction reactions with enhanced catalytic performances. Science China Materials, 2018, 61, 728-736.	3.5	203
41	Preparation and enhanced structural integrity of electrospun poly(ε-caprolactone)-based fibers by freezing amorphous chains through thiol-ene click reaction. Colloids and Surfaces A: Physicochemical and Engineering Aspects, 2018, 538, 7-13.	2.3	52
42	Fabrication of hierarchical MXene-based AuNPs-containing core–shell nanocomposites for high efficient catalysts. Green Energy and Environment, 2018, 3, 147-155.	4.7	60
43	Sandwiched Fe ₃ O ₄ /Carboxylate Graphene Oxide Nanostructures Constructed by Layer-by-Layer Assembly for Highly Efficient and Magnetically Recyclable Dye Removal. ACS Sustainable Chemistry and Engineering, 2018, 6, 1279-1288.	3.2	283
44	Self-Assembled Hydrogels Based on Poly-Cyclodextrin and Poly-Azobenzene Compounds and Applications for Highly Efficient Removal of Bisphenol A and Methylene Blue. ACS Omega, 2018, 3, 11663-11672.	1.6	56
45	Self-assembled MXene-based nanocomposites via layer-by-layer strategy for elevated adsorption capacities. Colloids and Surfaces A: Physicochemical and Engineering Aspects, 2018, 553, 105-113.	2.3	88
46	Preparation and adsorption capacities evaluation of supramolecular two-component gels nanostructures via fluorine-containing diacid and glutamic acid amino derivative. Integrated Ferroelectrics, 2018, 189, 135-146.	0.3	2
47	Self-Assembled AgNP-Containing Nanocomposites Constructed by Electrospinning as Efficient Dye Photocatalyst Materials for Wastewater Treatment. Nanomaterials, 2018, 8, 35.	1.9	126
48	Self-Assembled Composite Langmuir Films via Fluorine-Containing Bola-Type Derivative with Metal Ions. Coatings, 2018, 8, 141.	1.2	1
49	Facile preparation and electrochemical characterization of self-assembled core-shell diamond-polypyrrole nanocomposites. Colloids and Surfaces A: Physicochemical and Engineering Aspects, 2018, 555, 787-794.	2.3	15
50	Preparation of MoS ₂ -based polydopamine-modified core–shell nanocomposites with elevated adsorption performances. RSC Advances, 2018, 8, 21644-21650.	1.7	19
51	Graphene Oxide-Polymer Composite Langmuir Films Constructed by Interfacial Thiol-Ene Photopolymerization. Nanoscale Research Letters, 2017, 12, 99.	3.1	83
52	Bioinspired Polydopamine Sheathed Nanofibers Containing Carboxylate Graphene Oxide Nanosheet for High-Efficient Dyes Scavenger. ACS Sustainable Chemistry and Engineering, 2017, 5, 4948-4956.	3.2	224
53	Preparation of TiO2 nanoparticles modified electrospun nanocomposite membranes toward efficient dye degradation for wastewater treatment. Journal of the Taiwan Institute of Chemical Engineers, 2017, 78, 118-126.	2.7	44
54	Construction and self-assembly of beta-cyclodextrin derivative composite Langmuir films: Host-guest reaction and nanostructures. Colloids and Surfaces A: Physicochemical and Engineering Aspects, 2017, 533, 68-75.	2.3	10

#	Article	IF	CITATIONS
55	Variable self-assembly and in situ host–guest reaction of beta-cyclodextrin-modified graphene oxide composite Langmuir films with azobenzene compounds. RSC Advances, 2017, 7, 41043-41051.	1.7	18
56	Facile fabrication of hierarchical diamond-based AuNPs-modified nanocomposites via layer-by-layer assembly with enhanced catalytic capacities. Journal of the Taiwan Institute of Chemical Engineers, 2017, 80, 614-623.	2.7	11
57	Protective effects of asiatic acid in a spontaneous type 2 diabetic mouse model. Molecular Medicine Reports, 2017, 16, 1333-1339.	1.1	16
58	Preparation of diamond-based AuNP-modified nanocomposites with elevated catalytic performances. RSC Advances, 2017, 7, 49923-49930.	1.7	15
59	Preparation and self-assembly of graphene oxide-dye composite Langmuir films: Nanostructures and aggregations. Colloids and Surfaces A: Physicochemical and Engineering Aspects, 2017, 529, 793-800.	2.3	21
60	Preparation and self-assembly of two-component organogels via hexafluoropropane amino derivative and different acids. Integrated Ferroelectrics, 2017, 182, 75-83.	0.3	1
61	Hierarchical AuNPs-Loaded Fe3O4/Polymers Nanocomposites Constructed by Electrospinning with Enhanced and Magnetically Recyclable Catalytic Capacities. Nanomaterials, 2017, 7, 317.	1.9	34
62	Cyclocarya paliurus extract activates insulin signaling via Sirtuin1 in C2C12 myotubes and decreases blood glucose level in mice with impaired insulin secretion. PLoS ONE, 2017, 12, e0183988.	1.1	26
63	Self-Assembly and Drug Release Capacities of Organogels via Some Amide Compounds with Aromatic Substituent Headgroups. Materials, 2016, 9, 541.	1.3	13
64	Interleukin 18 promotes myofibroblast activation of valvular interstitial cells. International Journal of Cardiology, 2016, 221, 998-1003.	0.8	24
65	Preparation and photocatalytic property of silver nanoparticles using cationic pyridine derivative. Integrated Ferroelectrics, 2016, 169, 15-21.	0.3	0
66	Preparation and dye removal capacities of porous silver nanoparticle-containing composite hydrogels via poly(acrylic acid) and silver ions. RSC Advances, 2016, 6, 110799-110807.	1.7	46
67	Facile Synthesis of Highly Crystalline <i>α</i> -Fe ₂ O ₃ Nanostructures with Different Shapes as Photocatalysts for Waste Dye Treatment. Science of Advanced Materials, 2016, 8, 1005-1009.	0.1	15
68	Preparation and Absorption Capacity Evaluation of Composite Hydrogels via Graphene Oxide and Multi-Amine Molecules. Science of Advanced Materials, 2016, 8, 1400-1407.	0.1	6
69	Facile Preparation of Silver Halide Nanoparticles as Visible Light Photocatalysts. Nanomaterials and Nanotechnology, 2015, 5, 20.	1.2	17
70	Preparation of Iron-Nickel Alloy Nanostructures via Two Cationic Pyridinium Derivatives as Soft Templates. Nanomaterials and Nanotechnology, 2015, 5, 25.	1.2	5
71	Tang-Nai-Kang Alleviates Pre-diabetes and Metabolic Disorders and Induces a Gene Expression Switch toward Fatty Acid Oxidation in SHR.Cg-Leprcp/NDmcr Rats. PLoS ONE, 2015, 10, e0122024.	1.1	14
72	Qiwei granules alleviates podocyte lesion in kidney of diabetic KK-Ay mice. BMC Complementary and Alternative Medicine, 2015, 15, 97.	3.7	8

#	Article	IF	CITATIONS
73	Preparation and adsorption capacity evaluation of graphene oxide-chitosan composite hydrogels. Science China Materials, 2015, 58, 811-818.	3.5	70
74	Self-Assembly Reduced Graphene Oxide Nanosheet Hydrogel Fabrication by Anchorage of Chitosan/Silver and Its Potential Efficient Application toward Dye Degradation for Wastewater Treatments. ACS Sustainable Chemistry and Engineering, 2015, 3, 3130-3139.	3.2	202
75	Development of Decellularized Aortic Valvular Conduit Coated by Heparin–SDF-1α Multilayer. Annals of Thoracic Surgery, 2015, 99, 612-618.	0.7	28
76	Photothermally-Induced Molecular Self-Assembly of Macroscopic Peptide-Inorganic Hybrid Films. Science of Advanced Materials, 2015, 7, 1701-1707.	0.1	5
77	Organogels via Gemini Amphiphile-Graphene Oxide Nanocomposites: Self-Assembly and Symmetry Effect. Science of Advanced Materials, 2015, 7, 1677-1685.	0.1	5
78	MicroRNA-92a Inhibition Attenuates Hypoxia/Reoxygenation-Induced Myocardiocyte Apoptosis by Targeting Smad7. PLoS ONE, 2014, 9, e100298.	1.1	59
79	Supramolecular Assembly and Nanostructures of a Series of Luminol Derivatives with Aromatic/Alkyl Substituted Groups in Langmuir-Blodgett Films. Journal of Nanoscience and Nanotechnology, 2014, 14, 4400-4404.	0.9	2
80	Investigation of Orderly Nanostructures and Assembly Modes of Binary Organogels via Glutamic Acid Amino Derivative and Different Fatty Acids. Integrated Ferroelectrics, 2014, 151, 31-41.	0.3	2
81	Transcatheter Aortic Valve Implantation Versus Surgical Aortic Valve Replacement. Annals of Thoracic Surgery, 2014, 97, 1120.	0.7	2
82	Binary organogels based on glutamic acid derivatives and different acids: Solvent effect and molecular skeletons on self-assembly and nanostructures. Colloids and Surfaces A: Physicochemical and Engineering Aspects, 2014, 447, 88-96.	2.3	15
83	Isoquercitrin activates the AMP–activated protein kinase (AMPK) signal pathway in rat H4IIE cells. BMC Complementary and Alternative Medicine, 2014, 14, 42.	3.7	25
84	Comparison of Graft Patency Between Off-Pump and On-Pump Coronary Artery Bypass Grafting: An Updated Meta-Analysis. Annals of Thoracic Surgery, 2014, 97, 1335-1341.	0.7	67
85	Remote ischemic preconditioning does not improve the clinical outcomes in patients undergoing coronary artery bypass grafting: A meta-analysis of randomized controlled trials. International Journal of Cardiology, 2014, 172, e36-e38.	0.8	10
86	Closure of patent foramen ovale and prevention of recurrent thromboembolic events. Catheterization and Cardiovascular Interventions, 2014, 84, 164-164.	0.7	1
87	Self-Assembly and Headgroup Effect in Nanostructured Organogels via Cationic Amphiphile-Graphene Oxide Composites. PLoS ONE, 2014, 9, e101620.	1.1	22
88	Guava leaf extracts promote glucose metabolism in SHRSP.Z-Leprfa/Izm rats by improving insulin resistance in skeletal muscle. BMC Complementary and Alternative Medicine, 2013, 13, 52.	3.7	26
89	Self-assembly of organogels via new luminol imide derivatives: diverse nanostructures and substituent chain effect. Nanoscale Research Letters, 2013, 8, 278.	3.1	30
90	Regulation of substituent groups on morphologies and self-assembly of organogels based on some azobenzene imide derivatives. Nanoscale Research Letters, 2013, 8, 160.	3.1	28

#	Article	IF	CITATIONS
91	Off-pump coronary artery bypass grafting does not increase the 1-year mortality compared to on-pump: A meta-analysis of randomized controlled trials. International Journal of Cardiology, 2013, 169, e93-e95.	0.8	5
92	Spacer effect on nanostructures and self-assembly in organogels via some bolaform cholesteryl imide derivatives with different spacers. Nanoscale Research Letters, 2013, 8, 406.	3.1	18
93	Transcatheter closure of patent foramen ovale does not reduce the risk of recurrent ischemic stroke versus medical therapy alone: A meta-analysis of randomized controlled trials. International Journal of Cardiology, 2013, 169, e106-e108.	0.8	5
94	Minimally invasive direct coronary artery bypass reduces the need for repeated revascularization at long-term follow-up compared with stenting: A meta-analysis. International Journal of Cardiology, 2013, 168, 5469-5471.	0.8	3
95	Interfacial assembly of a series of Cu(II)-coordinated Schiff bases complexes: orderly nanostructures and supramolecular chirality. Science China Technological Sciences, 2013, 56, 20-24.	2.0	5
96	Nanostructures and Self-Assembly of Organogels via Benzimidazole/Benzothiazole Imide Derivatives with Different Alkyl Substituent Chains. Journal of Nanomaterials, 2013, 2013, 1-8.	1.5	12
97	Self-Assembly, Interfacial Nanostructure, and Supramolecular Chirality of the Langmuir-Blodgett Films of Some Schiff Base Derivatives without Alkyl Chain. Journal of Nanomaterials, 2013, 2013, 1-9.	1.5	7
98	Self-Assembly and Soft Material Preparation of Binary Organogels via Aminobenzimidazole/Benzothiazole and Acids with Different Alkyl Substituent Chains. Journal of Nanomaterials, 2013, 2013, 1-11.	1.5	5
99	Electrochemiluminescent Detection of Hydrogen Peroxide via Some Luminol Imide Derivatives with Different Substituent Groups. Journal of Chemistry, 2013, 2013, 1-6.	0.9	2
100	Preparation and Photocatalytic Property of Gold Nanoparticles by Using Two Bolaform Cholesteryl Imide Derivatives. Journal of Dispersion Science and Technology, 2013, 34, 1675-1682.	1.3	6
101	Nanostructure and supramolecular assembly of binary mixed organogels via trigonal acids and bipyridine derivatives. International Journal of Nanomanufacturing, 2013, 9, 375.	0.3	0
102	The Effect of Heparin-VEGF Multilayer on the Biocompatibility of Decellularized Aortic Valve with Platelet and Endothelial Progenitor Cells. PLoS ONE, 2013, 8, e54622.	1.1	49
103	Nanostructures and Substituent Alkyl Chains Effect on Assembly of Organogels Based on Some Glutamic Acid Diethyl Ester Imide Derivatives. Current Nanoscience, 2013, 9, 536-542.	0.7	7
104	Supramolecular Gel and Nanostructures of Bolaform and Trigonal Cholesteryl Derivatives with Different Aromatic Spacers. Current Nanoscience, 2012, 8, 111-116.	0.7	29
105	Photoresponsive organogel and organized nanostructures of cholesterol imide derivatives with azobenzene substituent groups. Progress in Natural Science: Materials International, 2012, 22, 64-70.	1.8	39
106	Supramolecular Assembly and Headgroup Effect in Interfacial Organized Films (I): A Study of Some Bolaamphiphiles. Journal of Dispersion Science and Technology, 2011, 32, 1592-1598.	1.3	6
107	Supramolecular Assembly and Headgroup Effect in Interfacial Organized Films (II): A Study of Some Single Chain Amphiphiles. Journal of Dispersion Science and Technology, 2011, 32, 1599-1604.	1.3	0
108	Supramolecular Assemblies and Self-Sorting of a Series of Cu(II)-Coordinated Schiff Bases Complexes at the Air/Water Interface. Journal of Dispersion Science and Technology, 2010, 31, 1120-1127.	1.3	2